Electronic Supplementary Material (ESI) for Journal of Materials Chemistry C.

Supporting Information

Mode-locking Pulse Generation Based on Lead-free Halide Perovskite $CsCu_2I_3$ Micro-rods with High Stability

Haiqin Deng†[a], Xing Xu†[b], Fangqi Liu†[c], Qiang Yu[a,d], Bowang Shu[a], Zixin Yang[a], Sicong Zhu*[c], Qinglin Zhang*[b], Jian Wu*[a], Pu Zhou[a]

[a] *College of Advanced Interdisciplinary Studies, National University of Defense Technology, Changsha 410073, China.*

[b] *School of Physics and Electronics, Hunan University, Changsha, 410082, China.*

[c] *College of Science and Key Laboratory for Ferrous Metallurgy, Resources Utilization of Ministry of Education, Wuhan University of Science and Technology, Wuhan, 430081, China.*

[d] *i-Lab & Key Laboratory of Nanodevices and Applications & Key Laboratory of Nanophotonic Materials and Devices, Suzhou Institute of Nano-Tech and Nano-Bionics, Chinese Academy of Sciences, Suzhou, 215125, China*

Corresponding Author

**E-mail:* *wujian15203@163.com; qinglin.zhang@hnu.edu.cn; sczhu@wust.edu.cn*

† These authors contributed equally to this work.

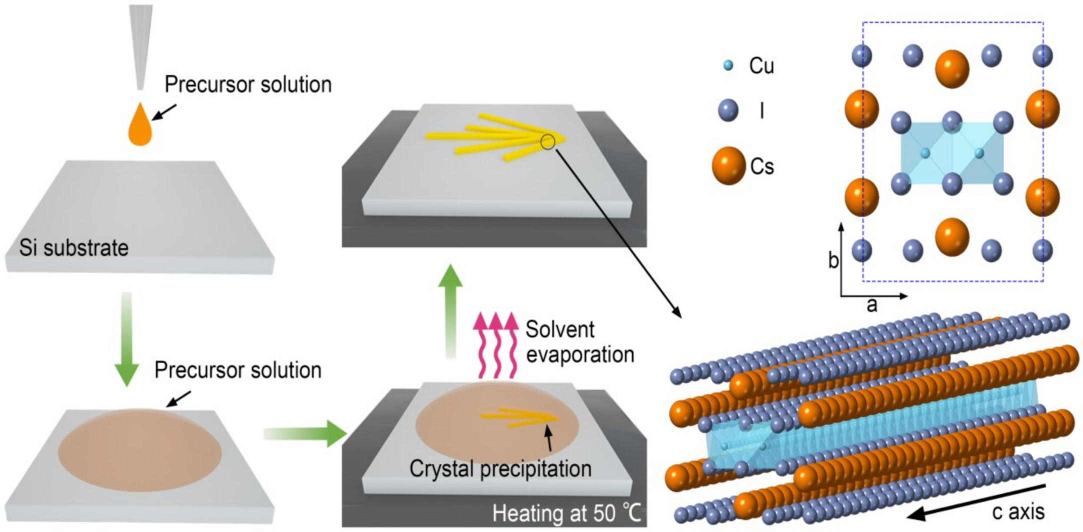

Figure S1. Characteristics of $CsCu_2I_3$ crystals: The schematic diagram of the $CsCu_2I_3$ micro-rods growth and the crystal structure of $CsCu_2I_3$.

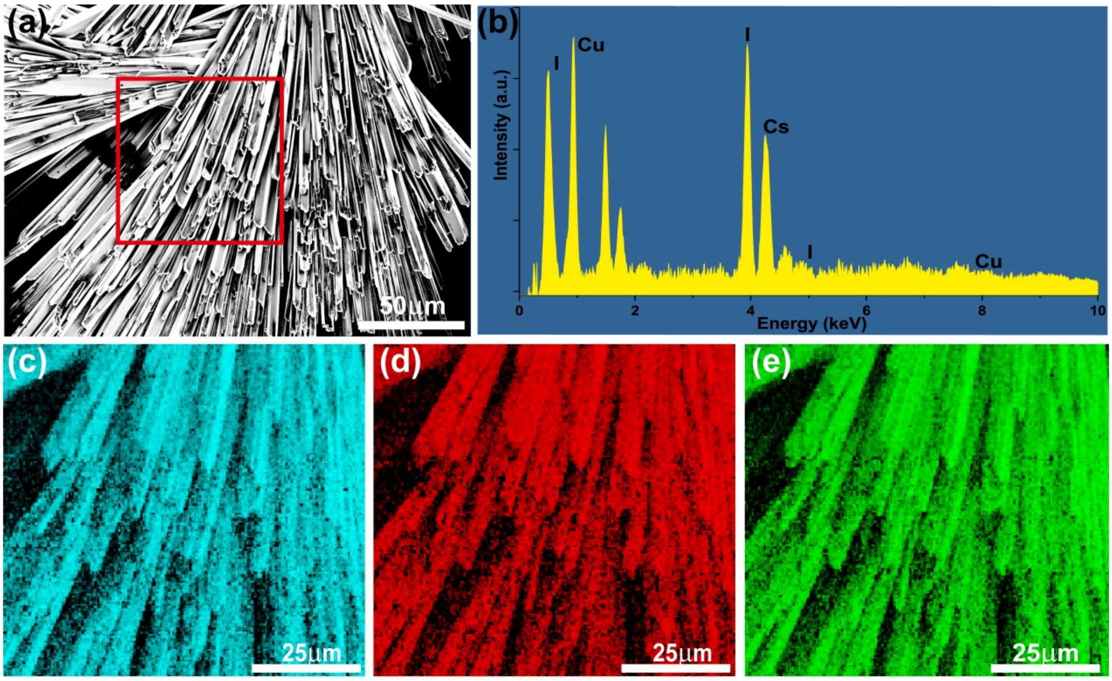

Figure S2. Crystal Characteristics of the $CsCu_2I_3$ micro-rods. (a) SEM image of the $CsCu_2I_3$ micro-rods. (b) EDS spectrum of the $CsCu_2I_3$ micro-rods sample. (c-e) Elemental mapping of Cs, Cu and I collected from the red square region in (a).

Fig. S2(a) displays the SEM image of the $CsCu_2I_3$ micro-rods grown on a silicon substrate. These rod-like structures possess uniform diameter and length. As shown in Fig. S2(b), the corresponding EDS spectra illustrates the sample contains Cs, Cu, and I (Si comes from the substrate) with an atomic ratio of about 1:2:3. The corresponding EDS elemental mapping images (Fig. S2(c-e)) demonstrated that these three elements were homogeneously distributed across the entire rods, indicating the uniform constituents of the obtained sample.

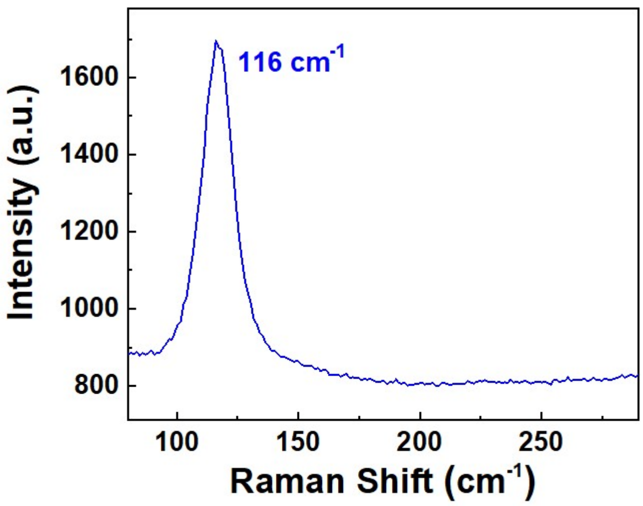

Figure S3. Raman spectrum of the $CsCu_2I_3$ micro-rods.

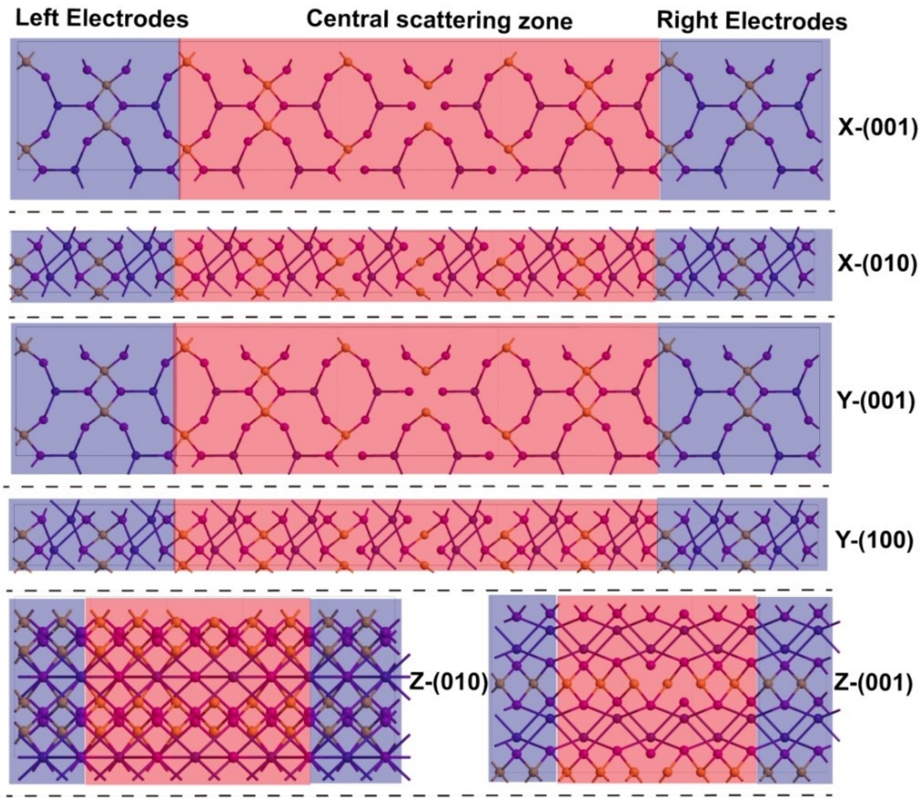

Figure S4. Schematic diagram of the optoelectronic device structure based on $CsCu_2I_3$ with different irradiation and transport directions.

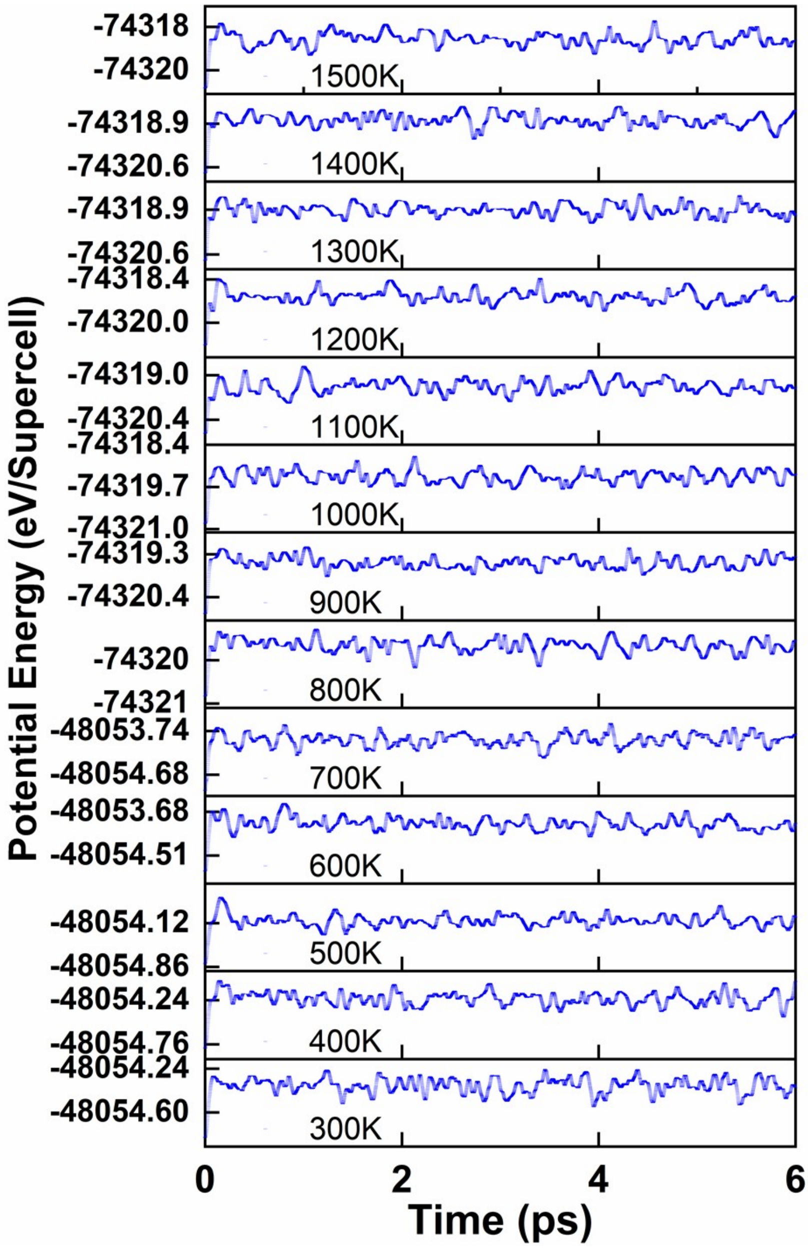

Figure S5. Variation of the potential energy of the system at different temperatures at 6ps.

44

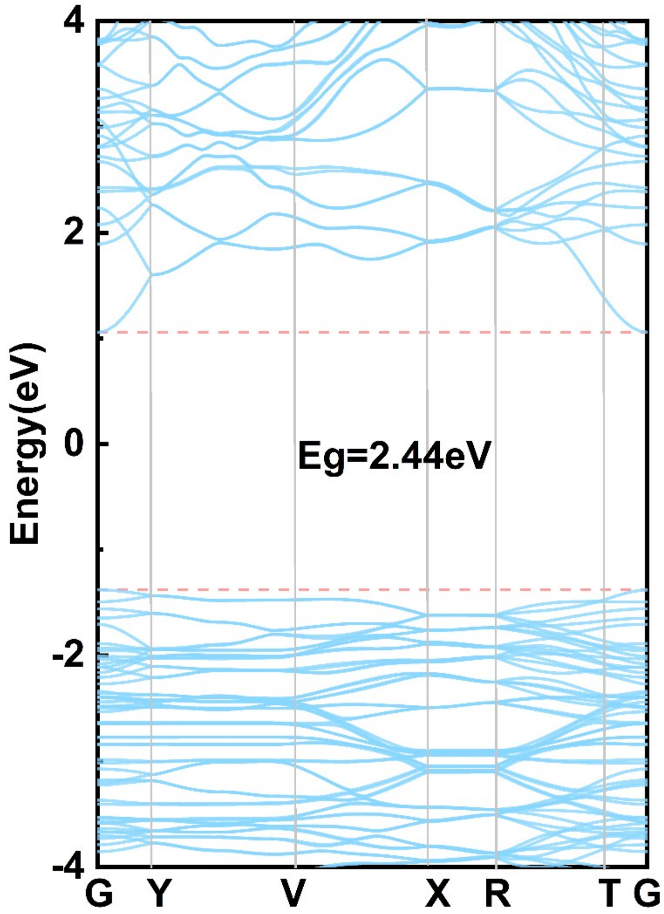

45 **Figure S6.** Electronic band structure of $CsCu_2I_3$.

Figure S7. The optical image of $CsCu_2I_3$ micro-rods on the fiber end-facet.

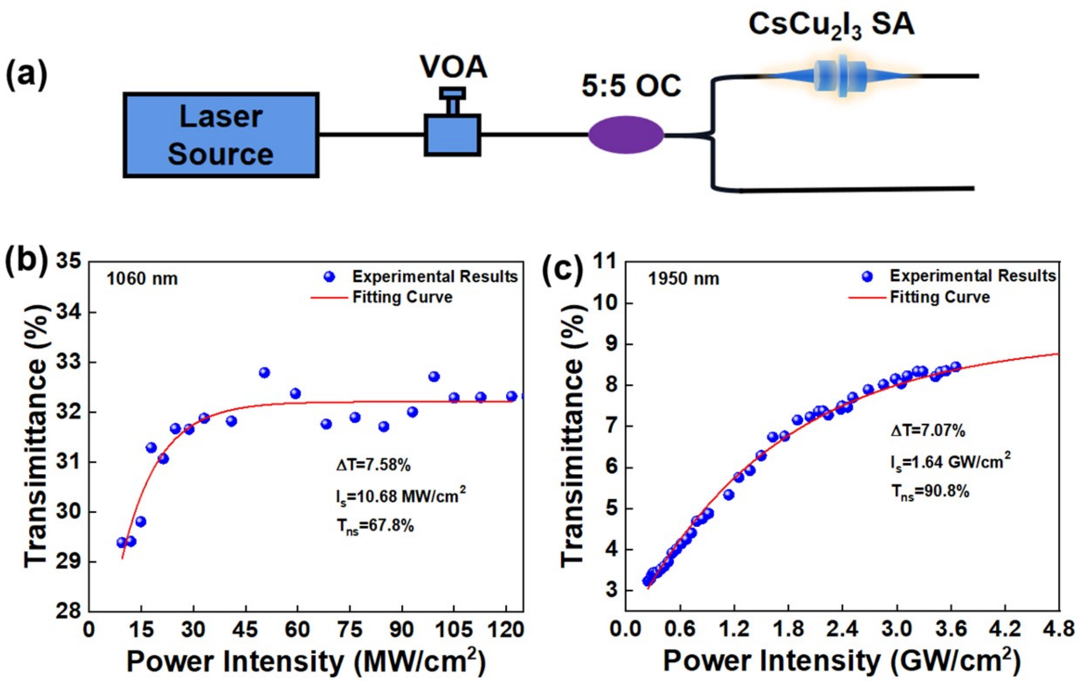

Figure S8. (a) The experimental measurement setup.The nonlinear optical properties of $CsCu_2I_3$ SA at (b)1060 nm and (c)1950 nm.

As exhibited in Fig. S8(a), the balanced twin-detector technique was used to measure the nonlinear properties of $CsCu_2I_3$ SA at 1 μm, 1.5 μm, and 2 μm. The laser source operated at 1060 nm/1550 nm/1950 nm with a repetition rate of 20 MHz/16.6 MHz/30MHz, and a pulse duration of 8 ps/ 448 fs/538 fs. The variable optical attenuator (VOA) was used to adjust the intensity of incident light. The 50/50 coupler was used to equally separate the incident light. Then, one passed through the $CsCu_2I_3$ SA, the other passed directly through the single-mode fiber. Finally, two power meters were used for testing the output power at the same time. In the nonlinear curves, the blue ball was the experimental data, and the solid red line was the fitting curve.

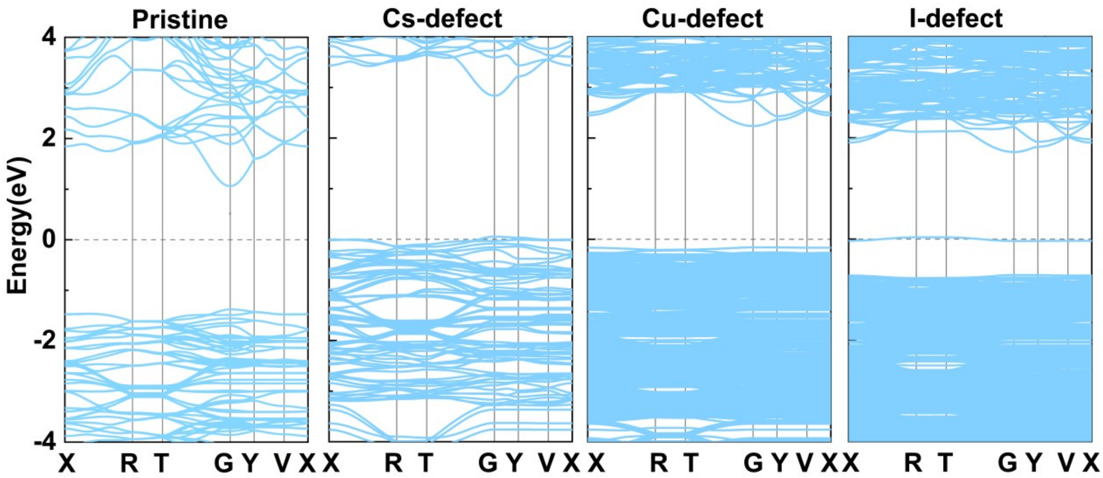

Figure S9. Electronic band structure of $CsCu_2I_3$ in the absence of defects in Cs, Cu, and I atoms.

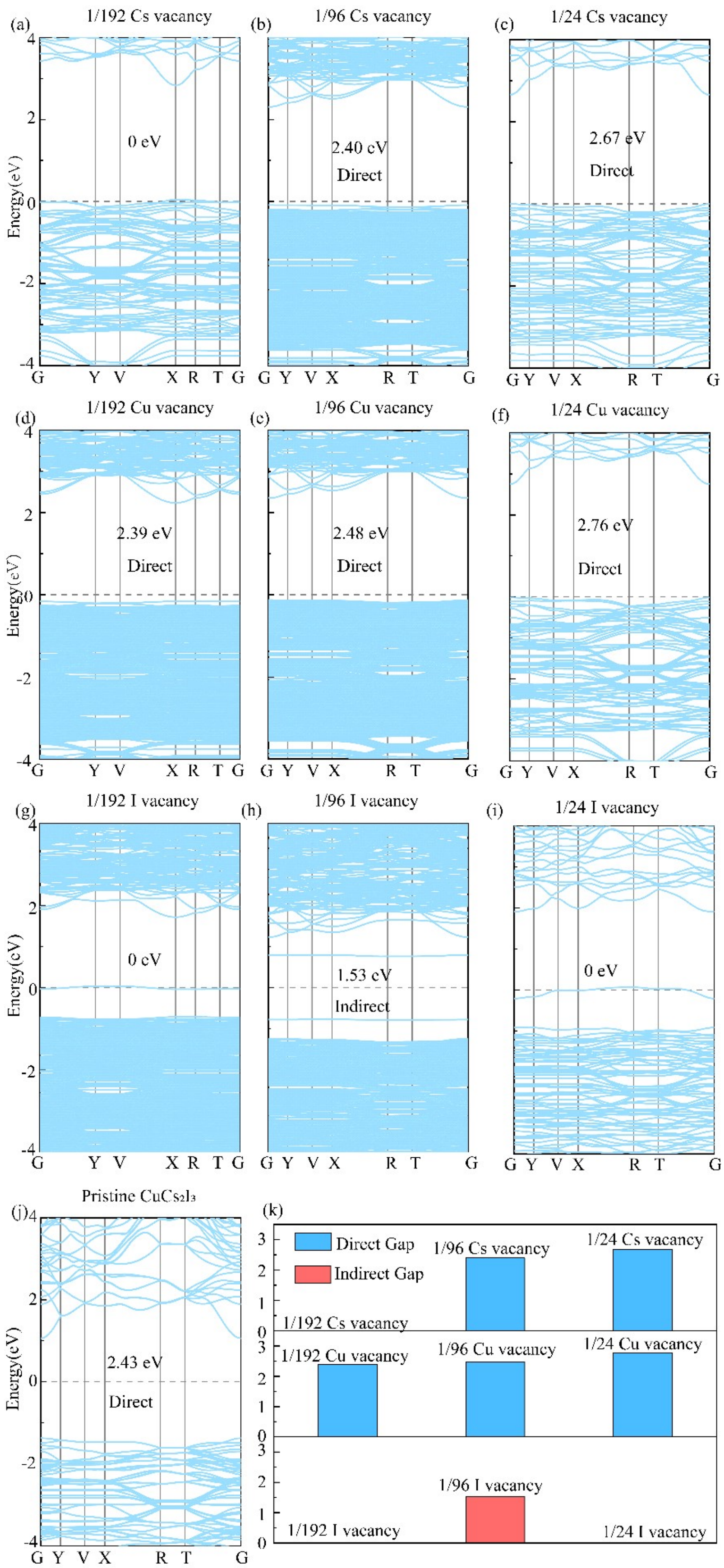

Figure S10. (a)-(i) $CsCu_2I_3$ based on different Cs, Cu, and I atomic vacancy concentrations. (j) Electronic band structures of pristine $CsCu_2I_3$. (k) Band gap variation with different Cs, Cu, and I atomic vacancy concentrations.

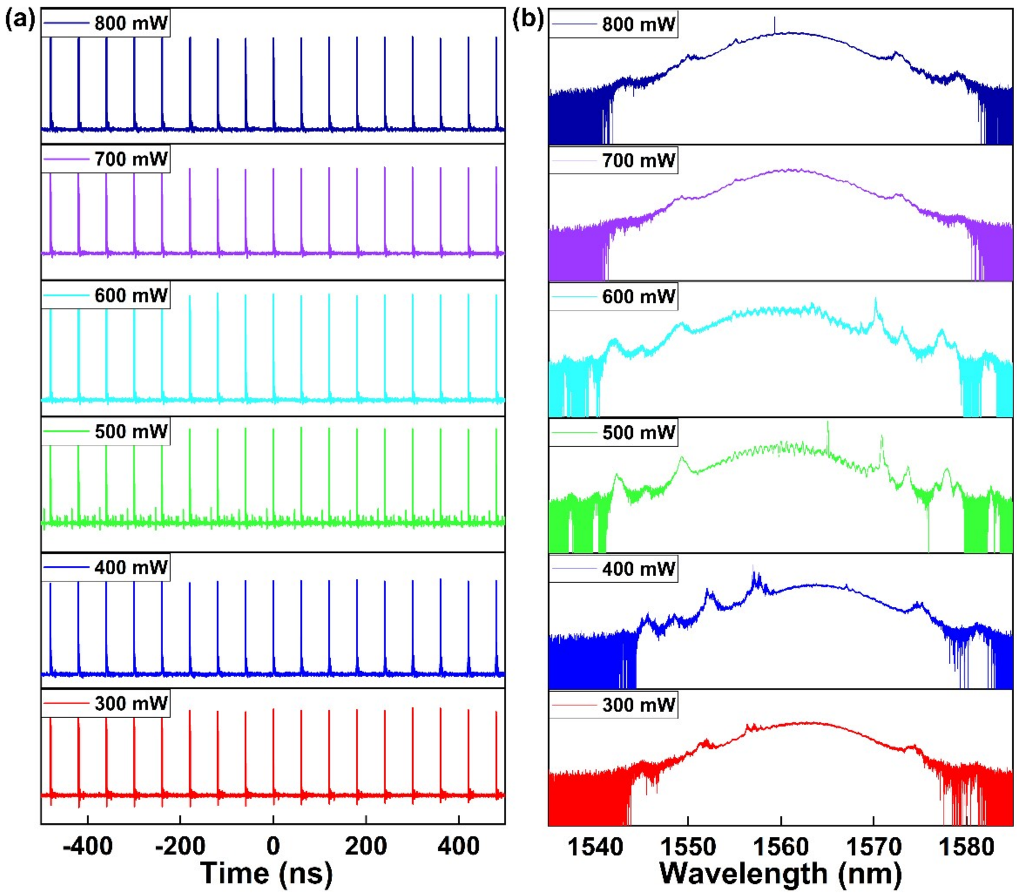

Figure S11. Experimental data of the 1st day. (a-b) Pulse train and spectrum of under different pump power.

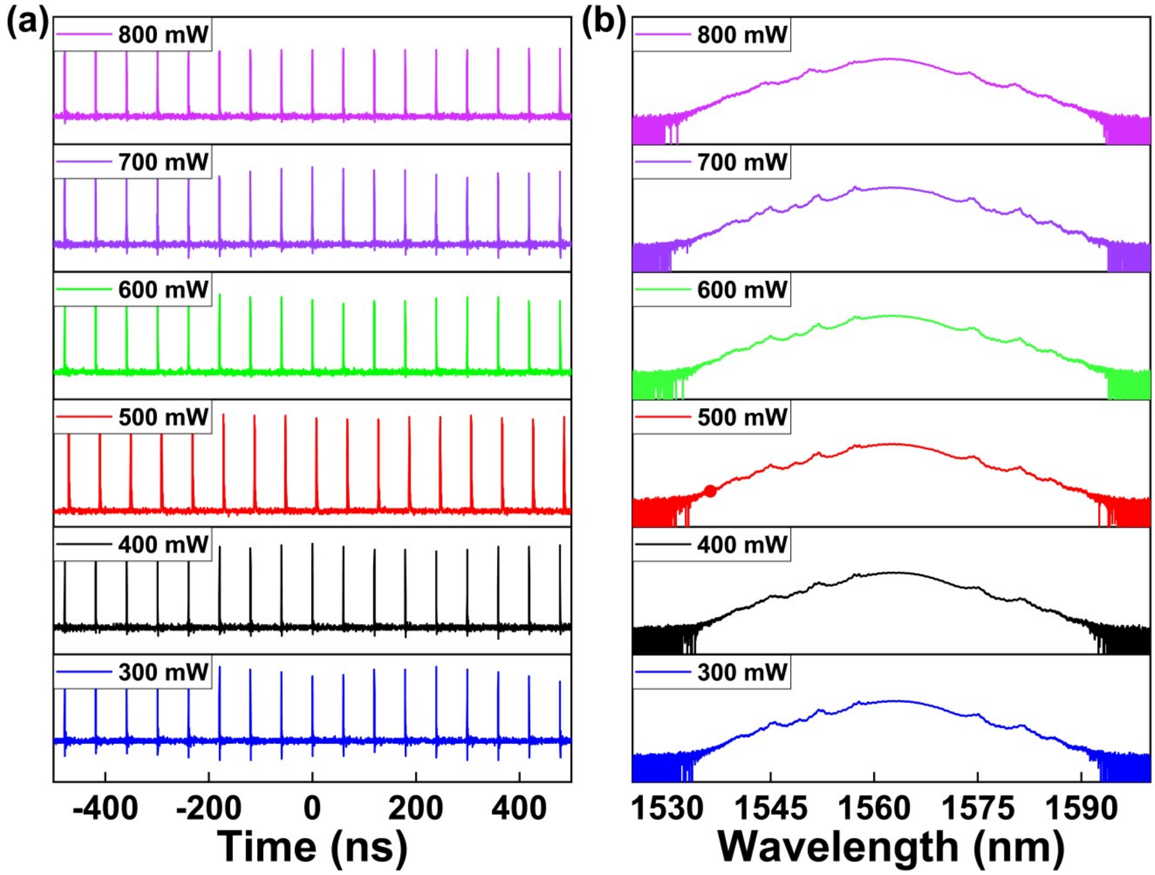

Figure S12. Experimental data of the 6th day. (a-b) Pulse train and spectrum of under different pump power.

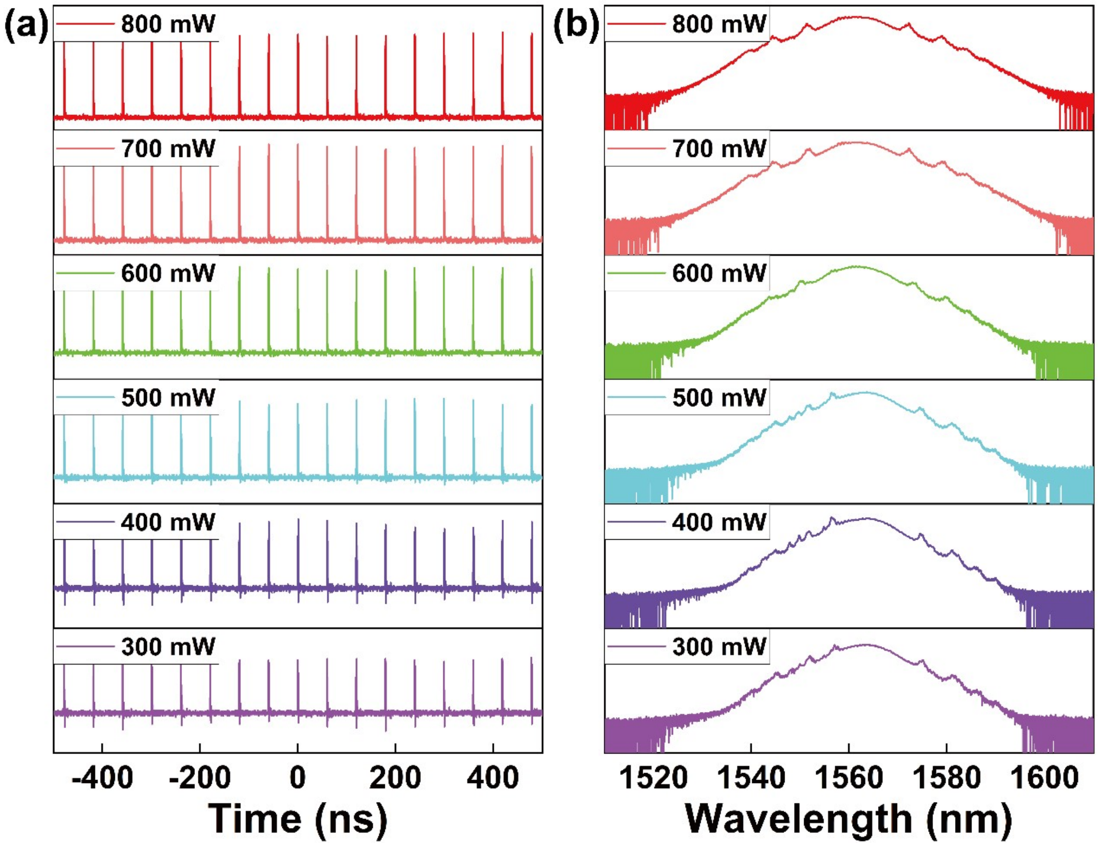

Figure S13. Experimental data of the 8th day. (a-b) Pulse train and spectrum of under different pump power.

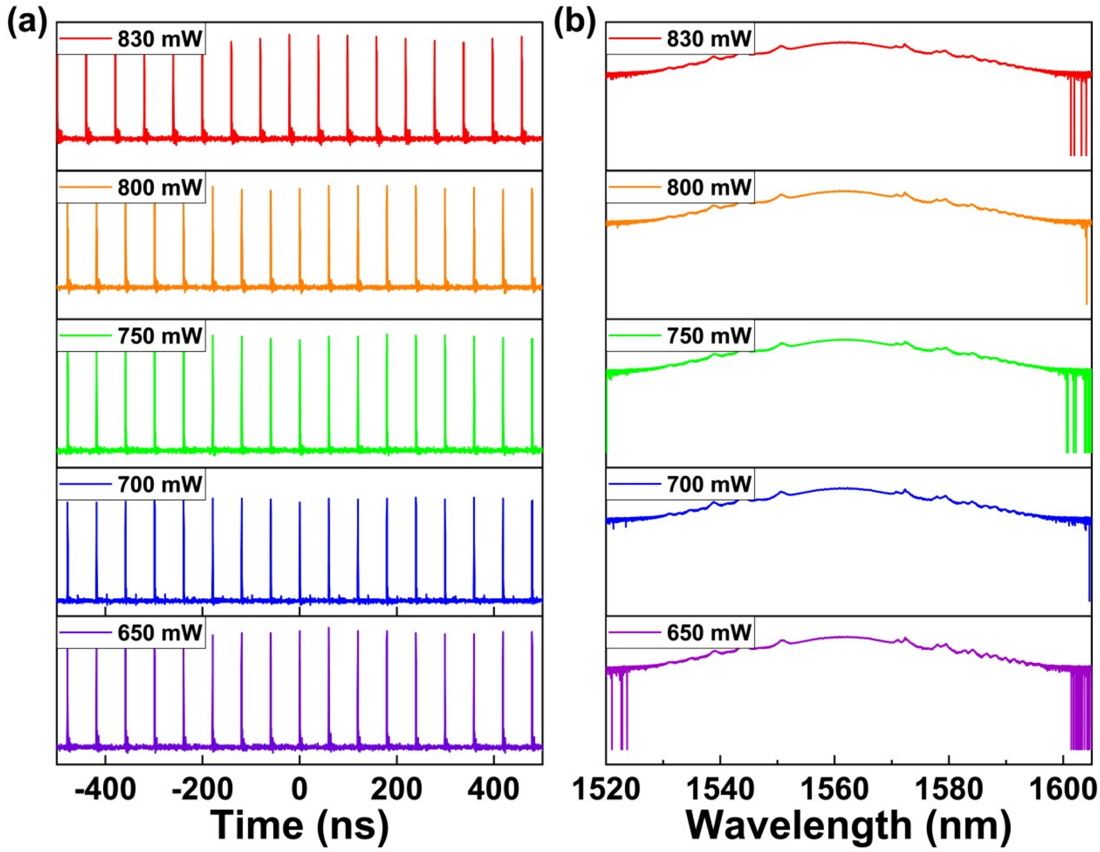

Figure S14. Experimental data of the 130th day. (a-b) Pulse train and spectrum of under different pump power.

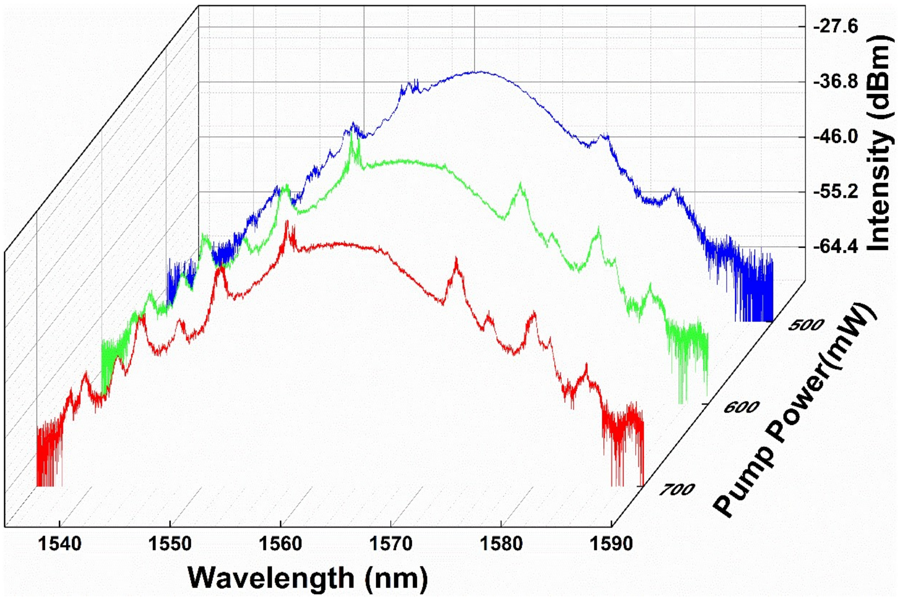

Figure S15. Experimental data of the 164th day, the spectrum of under different pump power.